SIGNIFICANCE OF TOPOGRAPHY-DRIVEN VERTICAL TRANSPORT ON THE GLOBAL WATER CYCLE ON MARS

R. A. Urata, *Bay Area Environmental Research/NASA Ames Research Center, Moffett Field, USA (richard.a.urata@nasa.gov)*, **M. Kahre, J. Hollingsworth**, *NASA Ames Research Center, Moffett Field, USA*.

Summary:

We use a 3D Mars general circulation model (GCM) to show that vertical transport of water is enhanced during northern summer due to influences from topography, such as mountain waves. Additionally, an increase in the vertical transport is seen when the resolution to 2°x3°. The finer resolution improves the ability to resolve terrain-induced circulation, and boosts the vertical transport of water. The increased vertical transport places water higher in the atmosphere leading to more ice mass in the aphelion cloud belt, and greater cross-equatorial water transport via the upper branch of the Hadley cell.

Introduction:

The "aphelion cloud belt" is a term used to describe the band of tropical clouds that form annually on Mars during the aphelion season *(L_s=0°-180°)*. The clouds tend to form high in the troposphere and influence the thermal structure of the tropics, thus the large-scale circulation during this season. The Hubble Space Telescope observed the clouds in the mid-1990's (Wolff et al., 1999), and the Thermal Emission Spectrometer (TES) aboard the Mars Global Surveyor (MGS) made long-term continuous observations and showed the seasonality of the clouds (Smith, 2004). Since 2006, the Mars Climate Sounder (MCS) on the Mars Reconnaissance Orbiter (MRO) has provided limb observations revealing the cloud tops to be relatively high in the atmosphere (Figure 1). More recently, observations of the spatial distribution of water vapor by the SPICAM spectrometer onboard Mars Express showed high degrees of supersaturation in the upper atmosphere not usually seen in models (Maltagliati et al., 2013).

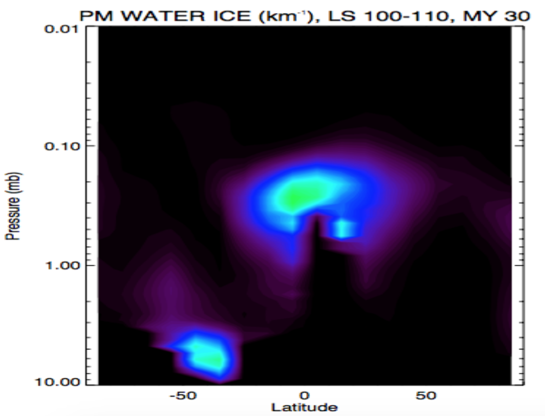

Figure 1. Vertical cross section of cloud opacity per km around L_s=105° from MCS.

The question is then how water can be transported to the upper regions of the atmosphere to be able to form high clouds. Using a non-hydrostatic mesoscale Mars atmospheric model, Michaels, et al. (2006) showed that there is significant vertical transport of water by topographically-induced circulations to altitudes otherwise unattainable. Their study focused on the Tharsis Montes region of Mars, and ran for several sols around L_s=100° at a horizontal resolution of approximately 40 km. It was found that the mountains caused thermally-driven slope flows and mountain waves, pushing water and ice tens of kilometers up into the atmosphere, and concluded that this transport is likely an important part of the global circulation.

Model Description:

For this study we use the NASA Ames Mars General Circulation Model (Haberle et al., 1999). The model is run at a typical resolution of 5°x6° with 24 vertical layers. The radiative transfer is a two-stream k-coefficient scheme with gaseous absorption and scattering aerosols, including dust and water ice. Tracer microphysics includes nucleation, growth, settling of cloud particles, as well as tracer mixing and sedimentation. The boundary layer scheme is based on the level-2 Mellor-Yamada formulation of turbulent mixing. Surface topography is based off of MOLA measurements, and Oregon State-derived surface albedo and thermal inertias are used. Tracer transport is done using a two-moment scheme assuming a log-normal size distribution. We specify an effective standard deviation (σ_{eff}), transport tracer mass, and number density. We can use these values to derive the effective radius (r_{eff}). The model contains a temporally and spatially varying background dust based off of TES observations. If the dust opacity is lower than the observations, dust is injected into the bottom atmospheric layer at a rate of opacity 0.1/sol.

The key to the Michaels, et al. (2006) result was the ability to resolve the Tharsis Montes, and Olympus Mons in particular. However, even with a diameter of over 600 km, Olympus Mons is barely resolved at the nominal GCM resolution of 5°x6°, with 9 grid cells to represent the whole mountain. A horizontal resolution of 40 km to match Michaels, et al. (2006) would require a sub-degree global grid, which is not practical with the current model. Approaching this resolution required adding some flexibility to the model, especially considering model spin-up time requirements for the water cycle (at least one Mars year). For reference, with the current model running full physics, the model can simulate approximately 1 sol per hour of integration time at 2°x3°. At 1°x1°, this decreases to 2 model hours per hour of integration.

In order to get around this issue, we added the ability for the model to restart at a new horizontal resolution from files at any resolution. This allows us to spin up the model at nominal resolutions for a few Mars years, and then simulate a desired time frame at higher resolution. Since all of the simulations are restarted from the same set of files, this allows for a more direct comparison between the different model resolutions.

Results:

We present the results from two simulations, one with a resolution of 5°x6°, and the other with a resolution of 2°x3°. Both are restarted from L_s=60° from the second year of a spin up simulation run at 5°x6°. The results come from L_s=106°. Water ice clouds are radiatively active in both scenarios.

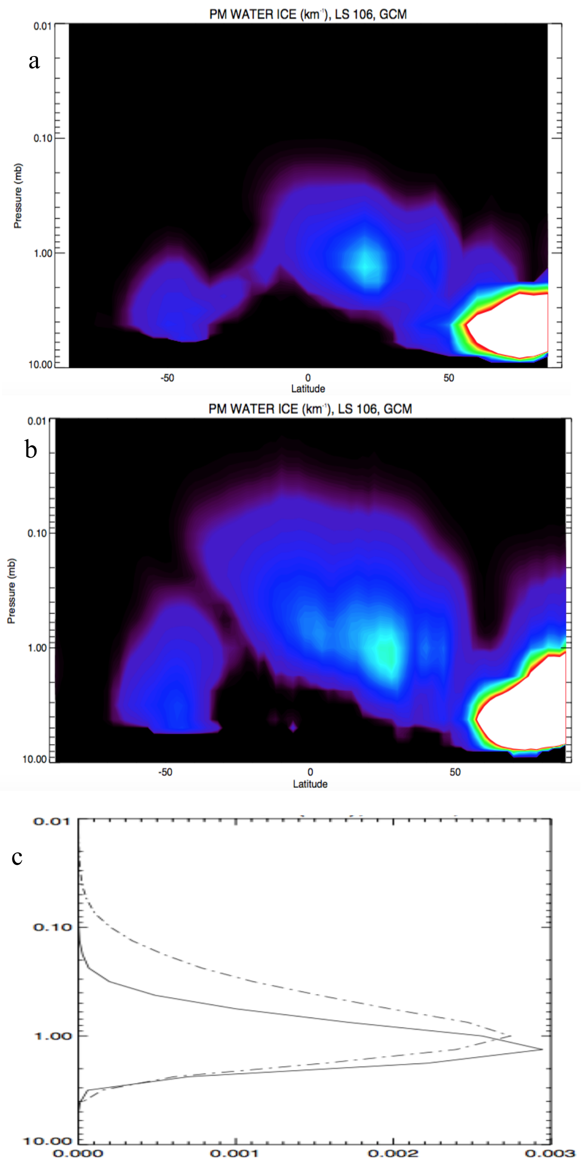

Figure 2. Zonal mean cloud opacity per km at L_s=106° at a resolution of (a) 5°x6°, (b) 2°x3°, and (c) a vertical profile at 20°N with 5°x6° in solid and 2°x3° in dot-dash.

A comparison between the two different resolutions for the zonal mean cloud opacity per km is given in Figure 2. The vertical extent of the tropical clouds is higher in the 2°x3° case, reaching up to the 0.1 mbar pressure level, while only reaching approximately the 0.4 mbar pressure level in the 5°x6° case. These plots show that the horizontal resolution has a dramatic effect on the aphelion cloud belt, and can potentially place water tens of kilometers higher in the atmosphere.

The cloud tops being higher in the 2°x3° case point to a large change in the transport of water. The immediate assumption would be that the Hadley cell circulation is more vigorous in the 2°x3° case. Figure 3 shows a comparison of the zonal mean mass stream function between the two cases. A simple qualitative comparison reveals however, that the strength of the Hadley cell is comparable in either case. This indicates that the process responsible for the vertical transport of water is not the general circulation, but a more local phenomenon.

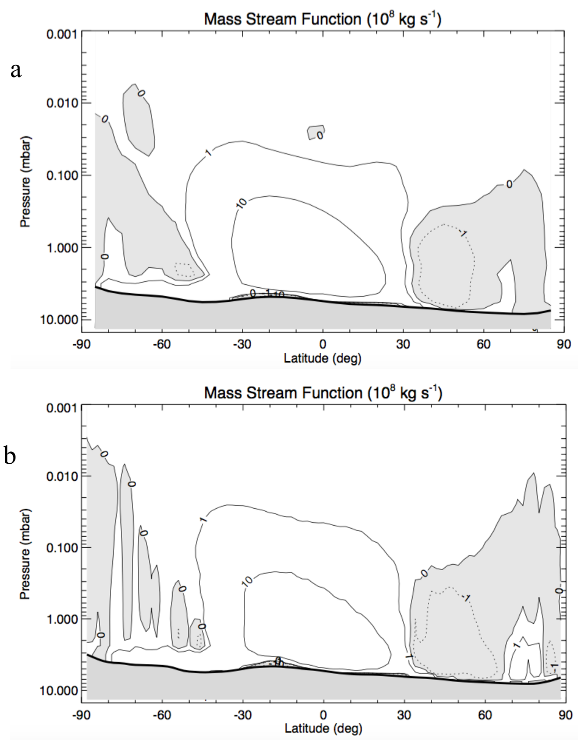

Figure 3. Zonal mean mass stream function at L_s=106° at a resolution of (a) 5°x6°, and (b) 2°x3°.

Since the vertical transport is not strongly associated with the zonal mean circulation, it is useful to look at the longitudinal variation of features. Figure 4 plots the daytime water ice cloud opacity at 12 microns in a latitude-longitude plot ranging from the equator to 50°N, with a topography contour overlay.

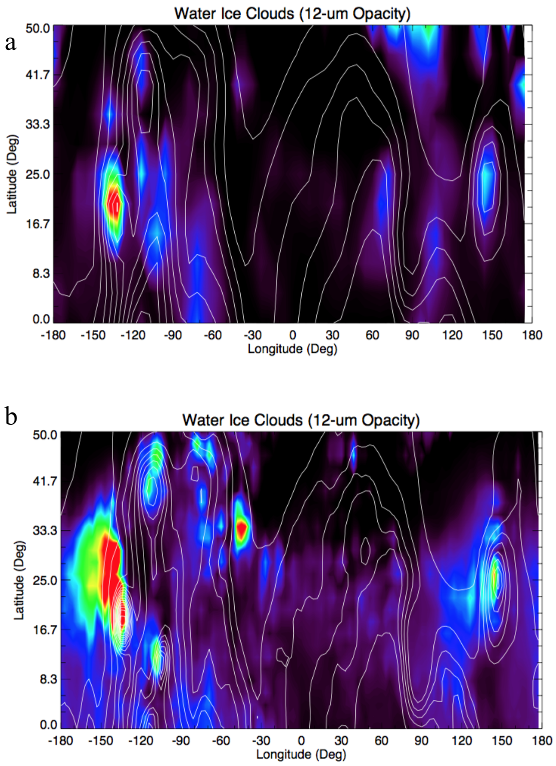

Figure 4. Latitude-Longitude plot of 12 micron cloud opacity with a topography contour overlay at a resolution of (a) 5°x6°, and (b) 2°x3°.

In both cases the most optically thick clouds are associated with high topography, mainly Olympus Mons. This is in agreement with Michaels, et al. (2006) who concluded that Olympus Mons plays a significant role in the transport of water.

During this time of year around L_s=100°, or northern summer, the general circulation is such that the return branch of the Hadley cell comes from the south, leading to easterly winds in the northern hemisphere. This means that the clouds around Olympus Mons and the other mountains are forming on the leeward side of the mountains.

When the wind encounters a large obstacle such as a large mountain, or mountain range, it is possible to create stationary gravity waves on the leeward side of the mountains. These flows can manifest as trapped waves if the wind speed above the flow increases significantly with height, or as vertically propagating waves if the wind speed increases slowly with height. Figures 5 and 6 show pressure-longitude vertical slice plots of the temperature and water ice clouds for the two resolutions, focusing on the area between -150°E to -90°E, at latitude = 20°N.

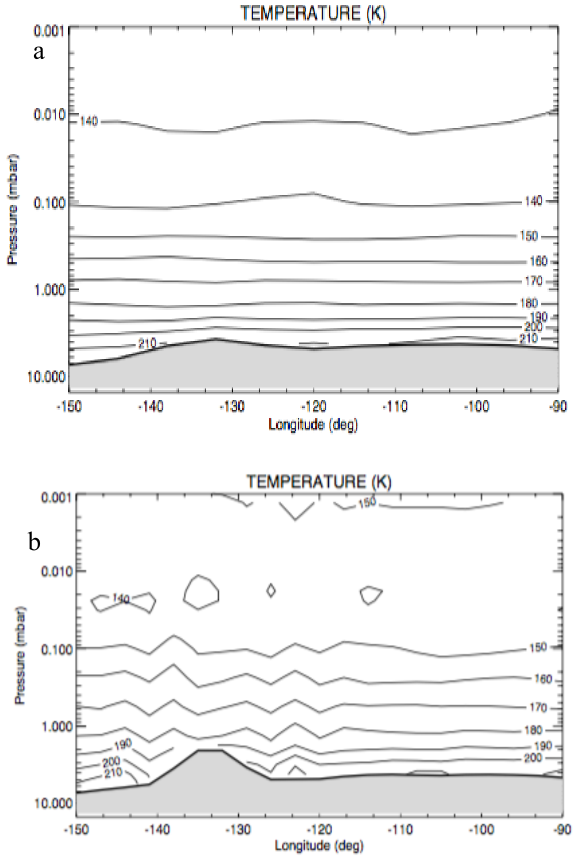

Figure 5. Pressure-longitude plots of temperature at L_s=106° at a resolution of (a) 5°x6°, and (b) 2°x3°.

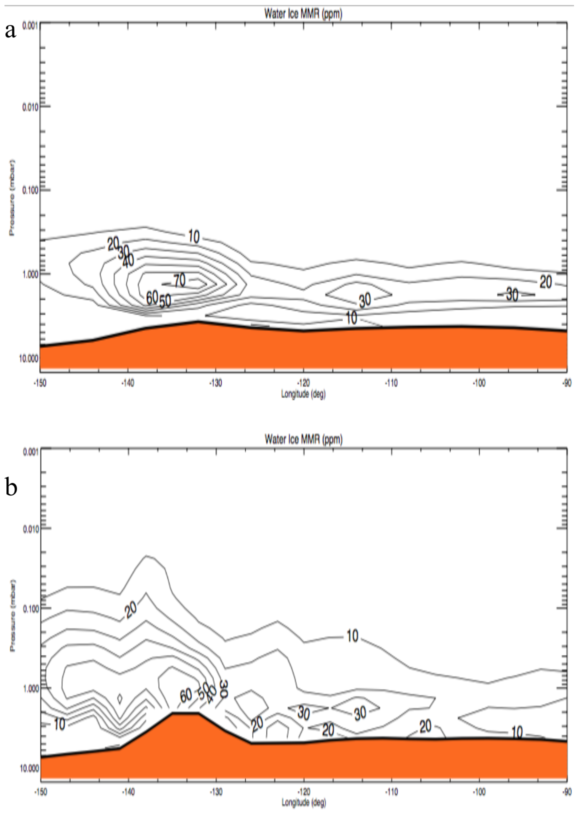

Figure 6. Pressure-longitude plots of water ice mixing ratio at L_s=106° at a resolution of (a) 5°x6°, and (b) 2°x3°.

Comparing the terrain between the two resolutions, it is clear that Olympus Mons (centered near -135°E) is more distinct in the 2°x3° case. In contrast, the mountain is barely visible in the coarser case. Because of this stark difference, it is not a surprise that mountain-induced circulations are much weaker in the 5°x6° results.

While no obvious mountain waves form in the 5°x6° simulations (Figs. 5a and 6a), there are distinct features in the 2°x3° simulations (Figs. 5b and 6b) indicating waves. The leeward temperature field in figure 5b displays characteristics of vertical propagating waves, and the water ice field has a strong peak above the mountain, which persists on the leeward side.

Conclusion:

Simulations of the Martian climate performed at two different resolutions (5°x6° and 2°x3°) indicate a significant increase in the mean vertical transport of water as resolution is increased. This has a large impact on the large-scale global transport of water, as it affects the total amount of water in the upper branch of the Hadley cell. The main source of the discrepancy is the ability (or inability) to resolve large terrain features such as Olympus Mons, the other Tharsis Montes, and Elysium Mons. These mountains greatly affect the mean circulation by introducing mountain waves and transporting copious amounts of water into the upper troposphere. We conclude that the mean circulation defined by the conventional Hadley cell transport is not sufficient to model all of the vertical transport of water, and that mountain-induced waves, which only manifest as strong influences at higher resolutions, are just as important, if not more. While there was a noticeable improvement in the height of the water in the transition to 2°x3°, the model results still do not match the observations. Additional testing is required to determine if the cloud placement will improve further at even higher resolutions, or if other parameterizations are necessary.

References:

Haberle, R., M. Joshi, J. Murphy, J. Barnes, J. Schofield, G. Wilson, M. Lopez-Valverde, J. Hollingsworth, A. Bridger, and J. Schaeffer (1999), General circulation model simulations of the Mars Pathfinder atmospheric structure investigation/ meteorology data, *Journal of Geophysical Research, 104(E4), 8957– 8974.*

Maltagliati, L., F. Montmessin, O. Korablev., A. Fedorova, F. Forget, A. Määtänen, F. Lefèvre, J.-L. Bertaux (2013), Annual survey of water vapor vertical distribution and water-aerosol coupling in the martian atmosphere observed by SPICAM/Mex solar occultations. *Icarus, 223, 942-962.*

Michaels, T.I., A. Colaprete, S.C.R. Rafkin, (2006), Significant vertical water transport by mountain-induced circulation on Mars. *Geophysical Research Letters, Vol.33, L16201, doi:10.1029/2006GL026562*

Smith, M.D., 2004. Interannual variability in TES atmospheric observations of Mars during 1999-2003. *Icaurs, 167, 148-165.*

Wolff, M.J., J.F. Bell III, P.B. James, R.T. Clancy, S.W. Lee (1999), Hubble Space Telescope observations of the Martian aphelion cloud belt prior to the Pathfinder mission: Seasonal and interannual variations, *Journal of Geophysical Research, 104(E4), 9027-9041.*